Molecular Plant Advance Access published November 29, 2011

RPL1, a Gene Involved in Epigenetic Processes Regulates Phenotypic Plasticity in Rice

Cui-Cui Zhang, Wen-Ya Yuan and **Qi-Fa Zhang**[1]

National Key Laboratory of Crop Genetic Improvement, National Center of Plant Gene Research, Huazhong Agricultural University, Wuhan 430070, China

ABSTRACT Organisms can adjust their phenotype in response to changing environmental conditions. This phenomenon is termed phenotypic plasticity. Despite its ubiquitous occurrence, there has been very little study on the molecular mechanism of phenotypic plasticity. In this study, we isolated a rice (*Oryza sativa* L.) mutant, *rice plasticity 1* (*rpl1*), that displayed increased environment-dependent phenotypic variations. *RPL1* was expressed in all tissues examined. The protein was localized in the nucleus and its distribution in the nucleus overlapped with heterochromatin. The *rpl1* mutation led to an increase in DNA methylation on repetitive sequences and a decrease in overall histone acetylation. In addition, the mutation affected responses of the rice plant to phytohormones such as brassinosteroid, gibberellin, and cytokinin. Analysis of the putative rice brassinosteroid receptor *OsBRI1*, a key hormone signaling gene, indicated that *RPL1* may be involved in the regulation of epigenomic modification of the gene. These data suggest that *RPL1* regulated phenotypic plasticity likely through its involvement in epigenetic processes affecting responses of the plant to phytohormones.

Key words: Phenotypic plasticity; *RPL1*; epigenetics; phytohormone; evolution.

INTRODUCTION

Living organisms struggle to adapt to their surroundings during their lifetime. The ability of an organism to change its phenotype in response to changes in environmental conditions was termed phenotypic plasticity (Price et al., 2003), which includes changes in an organism's characteristics in response to an environmental signal (Schlichting and Smith, 2002). It has been suggested that the mechanisms that enable the plastic responses, at protein production, physiological activity, growth, or behavior, are fundamentally the same (Schlichting and Smith, 2002; Via et al., 1995).

Two studies involving the heat-shock protein HSP90 showed that compromising HSP90 function released previously hidden genetic variation, resulting in novel phenotypes. In a study of *Drosophila melanogaster*, it was shown that, when the function of HSP90 was disrupted, phenotypic variation occurred in nearly all the structural characters of the adult fly (Rutherford and Lindquist, 1998). In *Arabidopsis*, reducing HSP90 function genetically or pharmacologically caused an array of morphological changes (Queitsch et al., 2002). This implies that HSP90 is a 'genetic buffer' or 'capacitor' of phenotypic variation (Queitsch et al., 2002; Rutherford and Lindquist, 1998). Generally, this sort of study is important for the understanding of complex relationships between genes, environment, and phenotypes (Pigliucci, 2002). Further studies showed that reduced activity of HSP90 induced a heritably altered chromatin state and suggested that HSP90 acted as a capacitor for morphological evolution through epigenetic and genetic mechanisms (Sollars et al., 2003). It was suggested that HSP90 might be required to regulate the assembly of multi-protein complexes such as the SWI/SNF complex for chromatin remodeling (Sangster et al., 2003). HSP90-mediated buffering systems offered an eloquent example of how epigenetic mechanisms might affect gene–environment interactions and showed that epigenetic variations might play a fundamental role in adaptation to rapidly changing environmental conditions (Pigliucci, 2003; Vercelli, 2004).

To probe phenotypic capacitors at a genomic scale, Lehner et al. (2006) tested more than 65 000 pairs of genes of *Caenorhabditis elegans* for their ability to interact genetically and identified six highly connected 'hub' genes: inactivation of these genes could enhance the phenotypic consequences of mutation of many different genes. All six hub genes encode components of chromatin modifying complexes (Lehner et al., 2006). Using high-throughput morphological phenotyping of individual yeast cells from single-gene deletion strains,

[1] To whom correspondence should be addressed. E-mail qifazh@mail.hzau.edu.cn, tel. 86-27-87282429, fax 86-27-87287092.

doi: 10.1093/mp/ssr091
Received 26 August 2011; accepted 5 November 2011

Levy and Siegal (2008) identified hundreds of genes in the genome that led to increased morphological variation when deleted. Approximately one-fourth of the identified capacitors in yeast are annotated to be involved in maintaining chromosome stability (Levy and Siegal, 2008). Tirosh et al. (2010) used gene expression profiling in engineered strains of two yeast species to show that chromatin regulators might act as capacitors for gene expression. Taken together, these findings indicate that most of the identified phenotypic capacitors are associated with chromatin and/or epigenetic processes.

Plants are sessile organisms that display great growth plasticity in responding to the changing environment (Callahan et al., 1997). The ability to modify stem elongation of plants in response to environmental cues is a classic form of adaptive phenotypic plasticity (Cipollini and Schultz, 1999). However, there has been very little study on the molecular mechanism of such phenotypic plasticity. In this work, we isolated a rice (*Oryza sativa* L.) mutant that showed increased environment-dependent plant height variations. This gene, designated *rice plasticity 1* (*RPL1*), encodes a nuclear protein of unknown function. The mutation altered the overall DNA methylation and histone modifications and affected plant response to several phytohormones such as brassinosteroid, gibberellin, and cytokinins. These data suggested that *RPL1* might play a role in epigenetic mechanisms regulating plant growth plasticity that may also involve plant hormone responses.

RESULTS

Identification of *rpl1* Mutant

In screening rice T-DNA insertional mutant library (Wu et al., 2003) in the paddyfield, we identified a semi-dwarf mutant numbered 03Z11UL95. Under normal growth conditions in the rice growing season in Wuhan, the mutant looked indistinguishable from the wild-type at the vegetative phase, but showed a semi-dwarf phenotype with small panicles at maturity stage (Figure 1A and 1B). The height (79.1 cm) of the mutant plant was 78.8% of that in wild-type (Table 1). Number of spikelets per panicle (114.3) was reduced by 32.9% in the mutant, due to a 13.2% reduction in number of primary branches and, to a larger extent, 49.7% reduction of secondary branches.

We numbered the internodes from top to bottom such that the uppermost internode was the first. Takeda (1977) described five types of dwarf mutants in rice based on the elongation pattern of the upper four to five internodes. The dn-type shows uniform shortening of all internodes, and the dm-type has a specific reduction in the second internode. In the d6-type, internodes below the uppermost are all shortened, while, in contrast, only the first internode is shortened in the sh-type. And the nl-type mutant has the longer fourth internode but with reduced first internode.

We surveyed the pattern of internode elongation of the mutant compared with wild-type and heterozygous plants, and

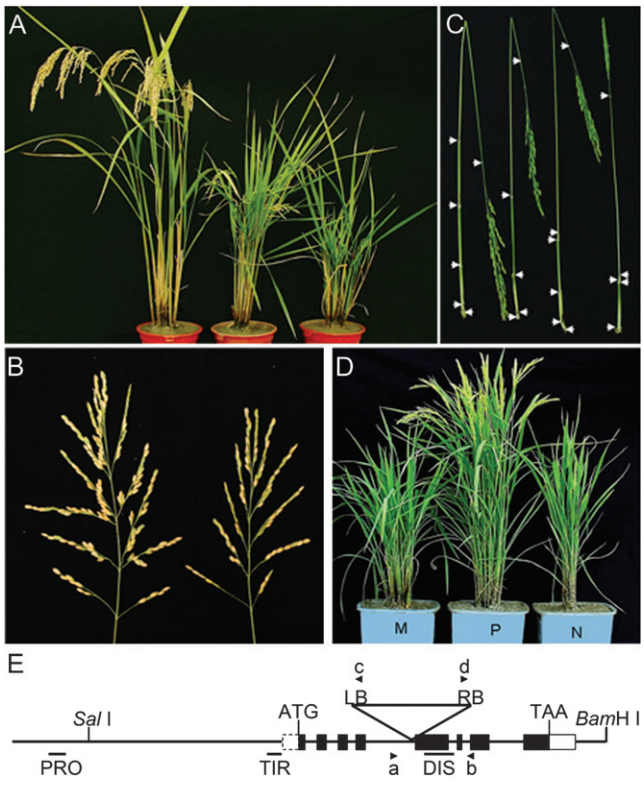

Figure 1. Identification of the *rpl1* Mutant.

(A) Morphology of a wild-type plant (left) and two *rpl1* mutant plants (right) at the maturity stage.

(B) Main panicles of wild-type (left) and mutant (right) plants.

(C) Elongation pattern of internodes. The wild-type plant (left) shows the normal elongation pattern, but culms of the *rpl1* mutant (right) show three types of internode elongation: the typical dn-, dm-type and another type specifically reducing second and third internodes. The white arrows indicate the nodes.

(D) Phenotype of the complementation test. Gross morphology at the vegetative phase of *rpl1* mutant (left), transgenic plant harboring the complementation construct (middle), and transgenic plant with an empty vector (right).

(E) Structure of *RPL1*. Eight exons (boxes) and seven introns (lines between boxes) are shown. T-DNA insertion site is located in the fourth intron. RB, right border; LB, left border of the T-DNA. The *Sal*I and *Bam*HI digestion sites indicate the DNA fragment introduced into mutant for the complementation test. Black bars at the bottom indicate the DNA region for bisulfite sequencing. Black arrowheads indicate the positions and orientations of the PCR primers for genotyping the T_1 plants and letters a–d stand for names of primers.

observed three internode elongation patterns in the mutant plants: dn- and dm-type plus one type of dwarfism not described by Takeda, in which both the second and third internodes were shortened (Figure 1C). These three types of culms were observed in different tillers of the same mutant plants, while all effective tillers in wild-type plants were normal.

We also planted the mutant in the winter nursery in Lingshui County (~18° N lat), Hainan Province, featuring a tropical moist monsoonal climate with short day length, compared to humid subtropical climate and long day length in summer rice

Table 1. Scores for Morphological Traits of Plants Grown in Summer Season in Wuhan 2009 or Winter Nursery in Lingshui 2008–09.

Source	Location	Number of plants	Plant height (cm)	Panicle length (cm)	Primary branch number per panicle	Secondary branch number per panicle	Number of spikelets per panicle	Tillers per plant
Wild-type	Wuhan	8	100.4 ± 1.4	22.7 ± 0.7	13.6 ± 0.4	33.4 ± 3.3	170.3 ± 10.0	26.5 ± 1.1
rpl1	Wuhan	8	79.1 ± 2.7	21.8 ± 0.6	11.8 ± 0.5	16.8 ± 2.7	114.3 ± 9.4	24.8 ± 1.2
P^a			1.42×10^{-5}	0.1636	0.0048	0.0008	0.0006	0.1528
rpl1/wild-type (%)			78.8	96.0	86.8	50.3	67.1	93.6
C51 with *RPL1*	Wuhan	6	98.2 ± 1.1	22.5 ± 0.2	15.7 ± 0.3	28.7 ± 2.0	168.8 ± 8.5	20.8 ± 1.2
C51 without *RPL1*	Wuhan	8	78.3 ± 3.2	18.8 ± 0.6	12.4 ± 0.5	11.1 ± 2.4	99.3 ± 8.5	23.9 ± 1.8
P^a			0.0001	0.0001	0.0001	5.86×10^{-5}	4.73×10^{-5}	0.0927
Wild-type	Lingshui	8	106.8 ± 2.2	18.4 ± 0.6	11.4 ± 0.5	32.8 ± 1.4	159.9 ± 4.5	9.8 ± 1.0
rpl1	Lingshui	6	47.4 ± 2.2	15.9 ± 1.1	7.8 ± 0.5	13.0 ± 1.9	74.0 ± 9.4	24.2 ± 3.6
P^a			2.28×10^{-10}	0.0349	0.0002	5.17×10^{-6}	3.06×10^{-5}	0.0048
rpl1/wild-type (%)			44.4	86.4	68.4	39.6	46.3	246.9
Location			33.35***	55.29***	43.37***	0.75	8.61**	23.88***
Genotype			338.24***	5.97*	33.47***	51.77***	67.63***	12.75**
Location × genotype			75.75***	1.43	3.17	0.38	3.00	20.78***

Data presented are mean ± s.e.m.
P^a-value from a *t*-test between the two genotypes.
*, **, and *** indicate the F-values are significant at 0.05, 0.01, and 0.001, respectively, based on a two-way ANOVA on these traits of wild-type and *rpl1* growing in Wuhan and Lingshui.

growing season in Wuhan (~30° N lat). All the traits measured of the wild-type plants, except tiller number, were not very different between Wuhan and Lingshui, indicating a stable phenotype. However, differences between mutant and wild-type were more dramatic in Lingshui than in Wuhan (Table 1). The scores of the mutant measured as percentage of the wild-type in Lingshui were greatly reduced for all morphological traits compared with the wild-type. The only exception was tiller number, which strikingly increased to approximately 2.5-fold in the mutant. A two-way analysis of variance (ANOVA) of these traits detected highly significant Location × Genotype interactions for plant height and tiller number (Table 1 and Supplemental Figure 1). This indicated that the mutant phenotype was more sensitive to environmental conditions than the wild-type. In other words, the mutant showed increased phenotypic plasticity, compared to the wild-type. We thus named this mutant *rice plasticity 1* (*rpl1*).

Identification of the *RPL1* Gene

The flanking sequence of the T-DNA insertion site was isolated and BLAST analysis showed that it was located in a putative gene (LOC_Os06g13640) on chromosome 6. Genotyping of T_1 plants showed that the T-DNA insertion site co-segregated with the semi-dwarf phenotype (Supplemental Figure 2). Analysis of the genomic sequence flanking the T-DNA insertion site indicated that this mutation was not allelic to known semi-dwarf mutants and apparently defined a novel locus that we designated as *rice plasticity 1* (*RPL1*).

Rapid amplification of the cDNA ends (RACE) and RT–PCR amplification showed that the ORF was 813 bp in length and the gene had eight exons and seven introns, in agreement with the sequence prediction. The T-DNA was inserted into the fourth intron leading to reduced expression of *RPL1* (Figures 1E and 2A). A PSI-BLAST of RPL1 failed to reveal any significant similarity to proteins in the protein databases, and InterPro Scan (www.ebi.ac.uk/Tools/InterProScan/) identified no putative domain in RPL1.

To further confirm that the *RPL1* mutation was responsible for the semi-dwarf phenotype, a 5461-bp genomic fragment containing the *RPL1* coding sequence, 2161 bp upstream of the translation initiation codon ATG and 516 bp downstream of the stop codon, was subcloned into the complementation construct and transformed into the mutant (Figure 1E). In total, 214 independent transgene-positive plants were generated, of which 154 showed restored plant height, whereas 28 plants transformed with a control vector that carried no rice genomic DNA showed no apparent improvement of plant height (Figure 1D). Southern blot hybridization analysis of nine phenotypically rescued T_0 transgenic plants chosen at random identified four plants harboring a single copy of the transgene, from which two transformants (C51 and C55) were chosen for further analysis. We grew a total of 183 T_2 plants of C51 and 219 T_2 plants of C55 for co-segregation analysis between the transgene and phenotype. All positive transgenic plants showed restored plant height, while all negative plants

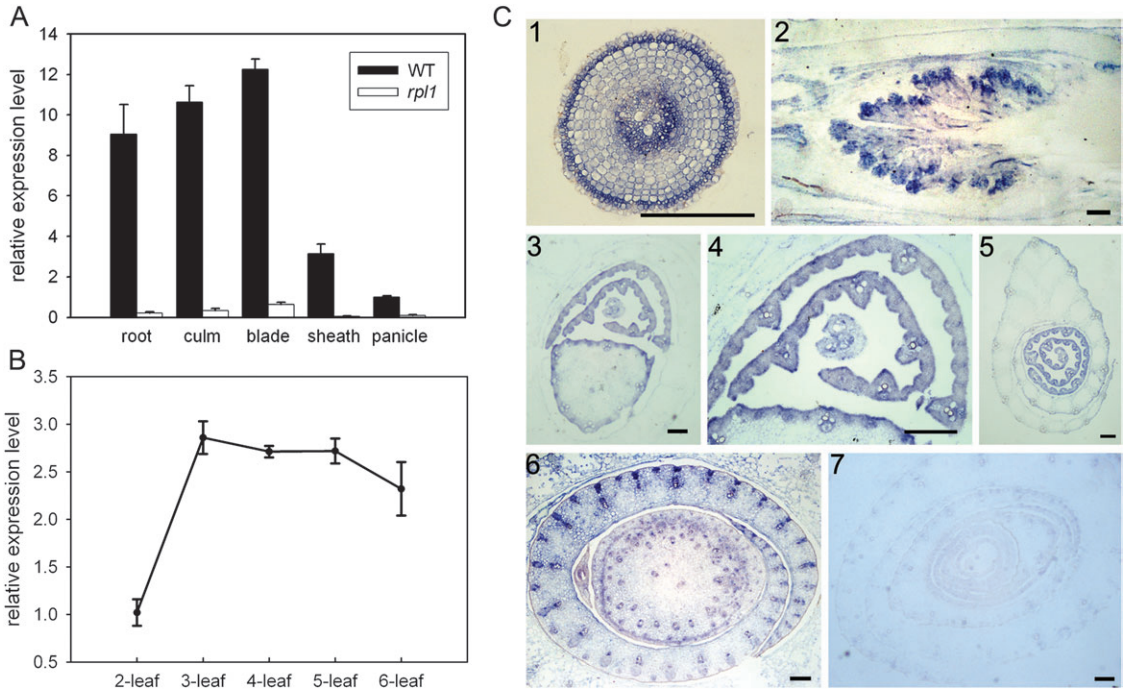

Figure 2. Expression Pattern of *RPL1*.

(A) Quantitative RT–PCR analysis of the expression pattern of *RPL1* in various tissues from wild-type and *rpl1* plants. The value for panicle of wild-type was arbitrarily set as 1. Error bars, s.e.m., based on three technical repeats.

(B) The relative expression level of *RPL1* in the third leaf of the wild-type seedlings at the two-to-six-leaf stages detected by quantitative RT–PCR analysis. Each sample was prepared from at least five seedlings. The value for the two-leaf stage was arbitrarily set as 1. Error bars, s.e.m., based on three technical repeats.

(C) *In situ* hybridization of various tissues from wild-type plants using an antisense probe. (1) Transverse section of root tip. (2) Longitudinal section of young panicle 2.5 mm in length. (3) Transverse section of the top internode in jointing stage. (4) Magnified image of part of (3). (5) Transverse section of a young tiller. (6) Transverse section of the bottom internode in jointing stage. (7) A negative control using the sense probe. Bar = 250 μm.

remained semi-dwarf (Supplemental Table 1). The progeny plants of C51 with or without introduced *RPL1* gene were examined for additional morphological traits. We found that plants with introduced *RPL1* gene totally restored the wild-type phenotype and those without the transgene remained mutant phenotype (Table 1). Therefore, we concluded that the insertional mutation at *RPL1* led to the semi-dwarf phenotype.

Expression Pattern of *RPL1*

Samples including root, culm, blade and sheath of flag leaf, and panicle were prepared from wild-type plants. The mRNA abundance of *RPL1* was detected using quantitative RT–PCR, which showed that *RPL1* was expressed in all tissues surveyed (Figure 2A). We monitored the *RPL1* transcript levels in the third leaf at each of the two-to-six-leaf stages of wild-type seedlings. At the two-leaf stage, the third leaf was small and tender and wrapped inside the second leaf sheath. At the three-leaf stage, the blade of third leaf was fully expanded and, at the four-leaf stage, its sheath fully extended. The third leaf began the aging process at the five-leaf stage and was almost completely senescent at the seven-leaf stage. The assay revealed that the *RPL1* transcript level in the third leaf was highest at the three-leaf stage and decreased gradually afterwards (Figure 2B).

RNA *in situ* hybridization experiment showed that the hybridization signal was detected in all tissues and enriched in vascular bundles and epidermis cells in root tip, culm, and leaf (Figure 2C). By comparing the signal intensity in Figure 2C(4–5), it was shown that hybridization signal in the youngest leaf was weaker than the surrounding older leaves but stronger than the outer mature leaf sheath.

Nuclear Localization of RPL1

To study subcellular localization of the RPL1 protein, a vector expressing a RPL1–ECFP fusion under the control of cauliflower mosaic virus (CaMV) 35S promoter was constructed (Figure 3A) and transformed into *Arabidopsis* mesophyll protoplasts. The RPL1–ECFP expression in the protoplasts was examined with confocal microscopy 10 h after transformation. The fluorescence showed that RPL1 is localized in the nucleus (Figure 3B).

We also assayed the localization using rice protoplast. The full-length *RPL1* coding sequence was translationally fused to the SUNLIGHTGFP-coding sequence under the control of the 35S promoter, which was transiently expressed in rice protoplasts isolated from *rpl1* etiolated seedlings. The fluorescence of the SUNLIGHTGFP could be distinguished from 4′,6-diamidino-2-phenylindole (DAPI) by a confocal

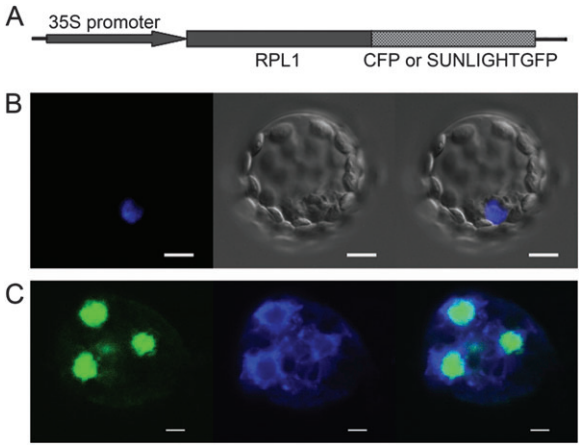

Figure 3. Subcellular Localization of RPL1 Protein.

(A) Diagram of the transient expression construct in which RPL1 is fused with a fluorescence protein.

(B) Nuclear localization of RPL1 in *Arabidopsis* protoplasts. Fluorescent image of ECFP (left); image in bright field (middle); merged image (right). The confocal images were acquired with a Zeiss LSM 510 Meta microscope. Bar = 10 μm.

(C) RPL1 distribution in rice nucleus. Fluorescent image of SUNLIGHTGFP (left); nucleus image stained with DAPI (middle); merged image (right). The confocal images were acquired with a Leica TCS SP2 microscope. Bar = 2 μm.

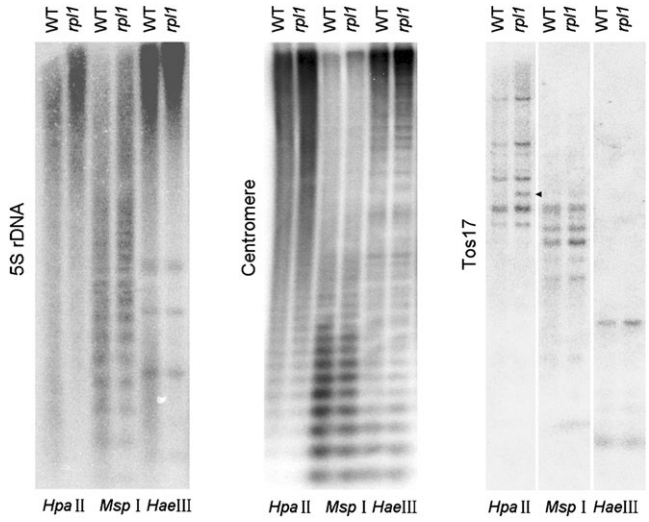

Figure 4. Southern Analysis of Methylation Patterns in Wild-Type and *rpl1*.

Approximately 3 μg genomic DNA was digested with *Hpa*II, *Msp*I, or *Hae*III electrophoresed in an 0.8% agarose gel, and transferred to a nylon membrane. The probes are indicated at left, and the black arrow indicates the extra band in *rpl1*.

microscope while the ECFP could not. Thus, both results showed that the RPL1 protein had a nuclear localization (Figure 3C).

Mutation in *RPL1* Affected Epigenetic Status

The significant phenotypic variation, or increased phenotypic plasticity, of the mutants in different growth environment suggested that *RPL1* might be involved in epigenetic processes. Chromatin modifications including DNA methylation and histone modifications are important in epigenetic regulation. DNA cytosine methylation in plants occurs at the CpG dinucleotide, CpNpG (where N is any nucleotide), and asymmetric CpHpH sites (where H is adenine [A], cytosine [C], or thymine [T]). Genome-wide mapping of cytosine methylation in rice shows that DNA methylation distribution pattern directly resembles the density distribution of repetitive DNA (Yan et al., 2010), a large portion of which is accounted for by the 180-bp centromere repeat family and the ribosomal RNA genes (Vongs et al., 1993). *Tos17* is a *copia*-like retrotransposon of rice, inactive (or almost inactive) under normal growth conditions accompanied by heavy DNA methylation (Hirochika et al., 1996; Liu et al., 2004).

To examine the DNA methylation pattern, genomic DNA prepared from leaves of wild-type and *rpl1* plants was digested with *Hpa*II, *Msp*I or *Hae*III and analyzed by Southern blots using 5S rDNA, centromere, and *Tos17* DNA as the probes. The results showed that there was a subtle change in methylation on 5S rDNA and centromere repeats in *rpl1*, as the mutant DNA showed slightly less digestion by *Hpa*II and *Msp*I (Figure 4), which may also be the case for *Hae*III digestion of 5S rDNA. Both *Hpa*II and *Msp*I recognize CCGG sequence, but neither can cleave m^5CCGG. Unlike *Hpa*II, *Msp*I can cleave Cm^5CGG. Although *Hae*III recognizes GGCC sequence, it cleaves GGCm^5C while GGm^5CC is resistant to cleavage. It is likely that the mutation increased cytosine methylation in the three sequence contexts. At the *Tos17* locus, an extra band was observed in the mutant DNA digested by *Hpa*II, indicating increased CpG methylation on *Tos17* in *rpl1*.

We also investigated modification changes of histones extracted from wild-type and *rpl1* seedlings (Figure 5), using Western blot analysis. The results showed that acetylation of H3 and H3K9 decreased substantially in the mutant, while other histone modification modules were not obviously affected. Because histone H3K9ac is associated with gene activation, decrease of this modification was in agreement with the increase in DNA methylation in the mutant.

RPL1 Also Modified Methylation Pattern of Its Own DNA

DNA methylation of *RPL1* gene was assayed using bisulfite sequencing. We prepared DNA from seedlings at the three-leaf stage and sequenced three fragments (Figure 1E): PRO, a 316-bp fragment from the promoter located in the region between –2330 and –2015 (the predicted transcription initiation site is indicated as +1); TIR, 106 bp in length in the putative transcription initiation region located between –131 and –26; and DIS, a fragment of 271 bp long located 125 bp downstream the T-DNA insertion site. The results showed that changes in DNA methylation level in *rpl1* were complex. The most noticeable differences were a large increase in the methylation level in the CG-context of the PRO fragment in

the mutant compared to the wild-type, and a similarly large decrease in the methylation level in the CG-context of the DIS fragment in the mutant relative to the wild-type (Table 2). These results suggested that the T-DNA insertion into *RPL1* changed the DNA methylation pattern of the *RPL1* gene itself.

Gibberellin and Cytokinin Signaling Pathways Were Affected in *rpl1*

Internode elongation of rice usually occurs only at the phase change of the shoot apical meristem from vegetative to reproductive stage, but exogenous GA_3 stimulation can induce internode elongation even in the juvenile phase (Ueguchi-Tanaka et al., 2000). We applied GA_3 treatment to wild-type and *rpl1* plants, and found that both plants began to elongate in 10^{-8} M GA_3, while in 10^{-5} M and 10^{-4} M concentrations mutant plant elongated faster than wild-type (Figure 6A). A recent

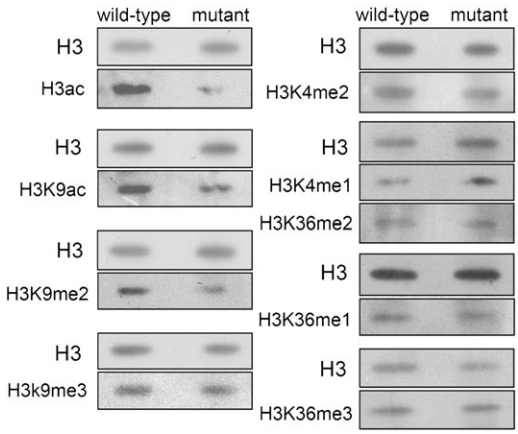

Figure 5. Western Blot Analysis of Histones Isolated from the Wild-Type and Mutant Plants.

Histone modification antibodies are indicated on the left. Antibodies against histone H3 (H3), Histone H3-acetylated K9 + K14 + K18 + K23 + K27 (H3ac), histone H3-acetylated K9 (H3K9ac), histone H3-dimethylated K9 (H3K9me2), histone H3-trimethylated K9 (H3K9me3), histone H3-monomethylated K4 (H3K4me1), histone H3-dimethylated K4 (H3K4me2), histone H3-monomethylated K36 (H3K36me1), histone H3-dimethylated K36 (H3K36me2), histone H3-trimethylated K36 (H3K36me3). Each of the eight membranes was hybridized using H3 antibody first, and then using the antibody below H3 in each panel.

study of Zhao et al. (2009) suggested that cytokinins (CK) influenced cell proliferation in emerging crown root primordia. When treated with serial concentrations of CK, crown root of wild-type plants decreased with the increase in the CK concentration, but *rpl1* plants seemed less sensitive to the treatment (Figure 6B).

Many enzymes of gibberellin (GA) metabolism have been identified, including CPS, GA20ox, and GA2ox (Hedden and Phillips, 2000; Yamaguchi, 2008). Os*GID1* encodes a soluble receptor for gibberellin (Ueguchi-Tanaka et al., 2005) and Os*SLR1* was the DELLA protein acting as a negative regulator of GA response (Ikeda et al., 2001). We performed a quantitative RT–PCR assay of *OsCPS1*, *OsGA20ox1*, *OsGA2ox1*, Os*GID1*, and Os*SLR1*, which showed remarkably elevated expression of all five genes in the mutant (Figure 6C), suggesting that the GA metabolism and signaling pathways were affected in *rpl1*.

The cytokinin signaling system involves sensor histidine kinase (HK) proteins, histidine phosphotransfer (HPt) proteins, and effector response regulator (RR) proteins (Kakimoto, 2003). Rice response regulator genes *OsRRs* represented the primary cytokinin response genes (Jain et al., 2006). We analyzed the expression levels of type-A *OsRR5* and *OsRR6* in plants at the early tillering stage, and detected a large increase in the transcript level of *OsRR5*, and a slight increase in *OsRR6* in the *rpl1* mutant compared to wild-type (Figure 6D). Hence, the cytokinin signaling pathway might be affected by *RPL1*.

Reduced Sensitivity of *rpl1* to Exogenous Brassinosteroid (BR) and the Relation to Changes in Histone Modification on *OsBRI1*

We also analyzed the response of the *rpl1* mutant to exogenous BR. The elongation of coleoptile and mesocotyl is a typical rice response to continuous darkness (Takano et al., 2001). Normally, coleoptile elongation stops at an early stage of germination in the dark in the absence of exogenously supplied BR, but elongates in the presence of exogenous BR (Yamamuro et al., 2000). When seeds were sown in culture media with a series of concentrations of BR in complete darkness, the coleoptile length of wild-type seedlings gradually increased after treatment, while the mutant showed no obvious increase and even a slight decrease with 0.1 μM BR (Figure 7A). Thus,

Table 2. Methylation of CG, CHG, and CHH Sites Checked by Bisulfite Sequencing in Wild-Type and *rpl1*.

Fragment	Length (bp)	Number of CG sites	Number of CHG sites	Number of CHH sites	Genotype	Methylation at CG site (%)	Methylation at CHG site (%)	Methylation at CHH site (%)
PRO	316	8	5	28	Wild-type	4.96	3.40	1.40
					rpl1	43.51	3.07	1.86
TIR	106	7	5	16	Wild-type	0.84	1.17	1.2
					rpl1	3.57	0	0
DIS	271	9	11	34	Wild-type	44.87	4.04	1.47
					rpl1	6.45	0.91	2.30

For every genotype, 20 sequenced clones were used for calculation for each fragment.

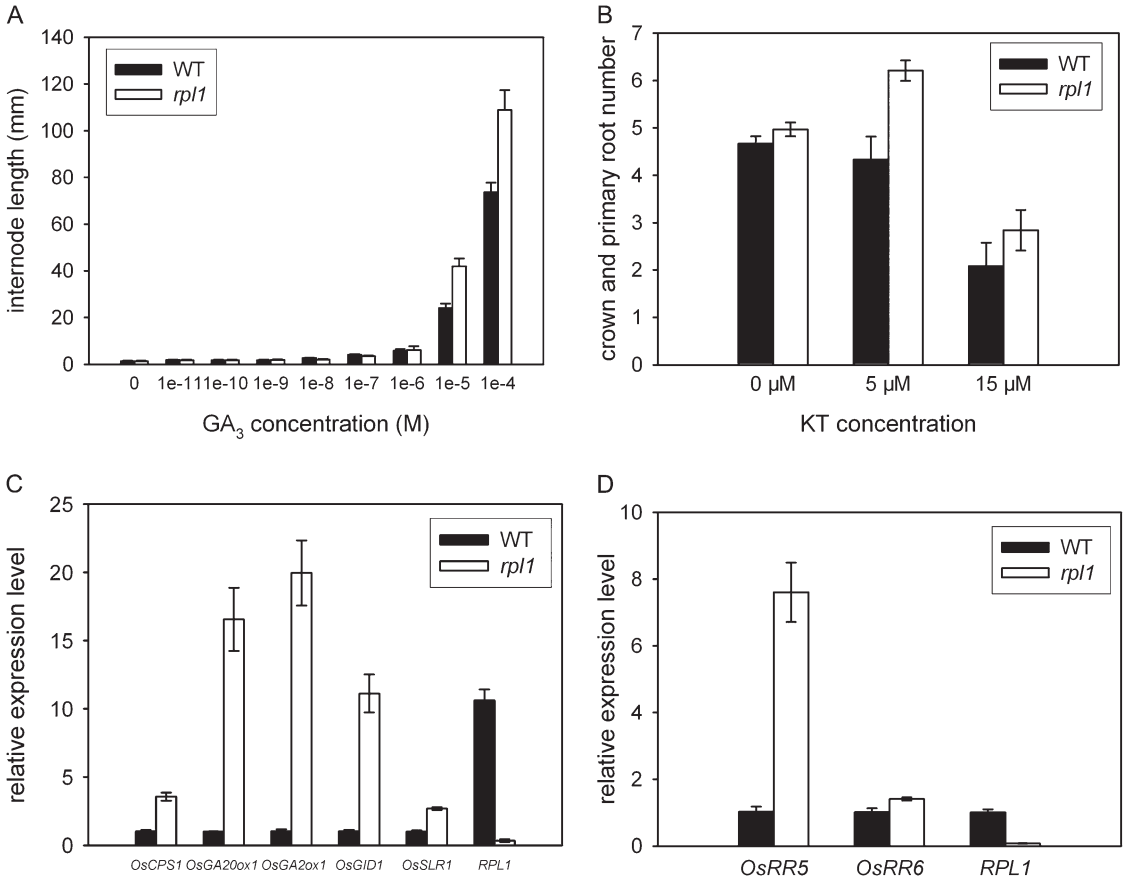

Figure 6. Responses of *rpl1* Mutant to Gibberellin (GA) and Cytokinin (CK) Treatments.
(A) Internode length of plants hydroponically cultured with series concentration of GA_3. Error bars, s.e.m., calculated from at least six plants.
(B) Crown and primary root number of seedlings grown in series concentration of KT. Error bars, s.e.m., calculated from at least 21 seedlings.
(C) Quantitative RT–PCR analysis of *OsCPS1*, *OsGA20ox1*, *OsGA2ox1*, *OsGID1*, *OsSLR1*, and *RPL1* in wild-type and *rpl1* plants. Culm samples prepared for *RPL1* expression pattern were used. Error bars, s.e.m., based on three technical repeats.
(D) Quantitative RT–PCR analysis of *OsRR5*, *OsRR6*, and *RPL1* in wild-type and *rpl1* plants at early tillering stage. Error bars, s.e.m., based on three technical repeats.

rpl1 seedlings were insensitive or much less responsive to exogenous BR than the wild-type in darkness.

Exogenous BR cannot affect coleoptile length of *d61*, which has a defective OsBRI1 (Yamamuro et al., 2000). To survey whether the mutant phenotype was associated with altered expression of BR-related genes, we tested the expression level of *OsBRI1*, which is homologous to the putative BR receptor gene *BRI1* in *Arabidopsis* (Yamamuro et al., 2000). In the *rpl1* mutant, the expression of *OsBRI1* was more than 100 times lower than in wild-type plants (Figure 7B). Thus, the reduced response of *rpl1* to exogenous BR might be accounted for by the extremely low expression of *OsBRI1*.

To study whether the *rpl1* mutation affected histone modifications of *OsBRI1*, chromatin immunoprecipitation (ChIP) assays with specific antibodies against histone H3K4me3, H3K36me3, and H3K9ac were performed. The precipitated DNA was analyzed by qRT–PCR using primer sets corresponding to two regions of *OsBRI1*. The results showed that the modifications of both H3K4me3 and H3K36me3 decreased on both regions of the gene in the mutant, together with an increase in modification of H3K9ac (Figure 7C).

DISCUSSION

RPL1 Was a Plasticity Gene Regulating Phenotypic Plasticity in Response to Growth Environments

Phenotypic plasticity is the ability of a single genotype to produce different phenotypes in response to environmental changes (West-Eberhard, 1989). Two classes of genes are generally recognized to possibly exist and act as plasticity gene: regulatory loci and environmentally sensitive alleles (Gutteling, 2004; Via et al., 1995). In this work, the increase in phenotypic variation of the mutant relative to the wild-type in different locations suggests that *RPL1* may be a regulatory gene that controls the phenotype stability or plasticity. The wild-type allele *RPL1* is associated with high phenotype stability, while the mutant allele causes reduced stability or increased plasticity.

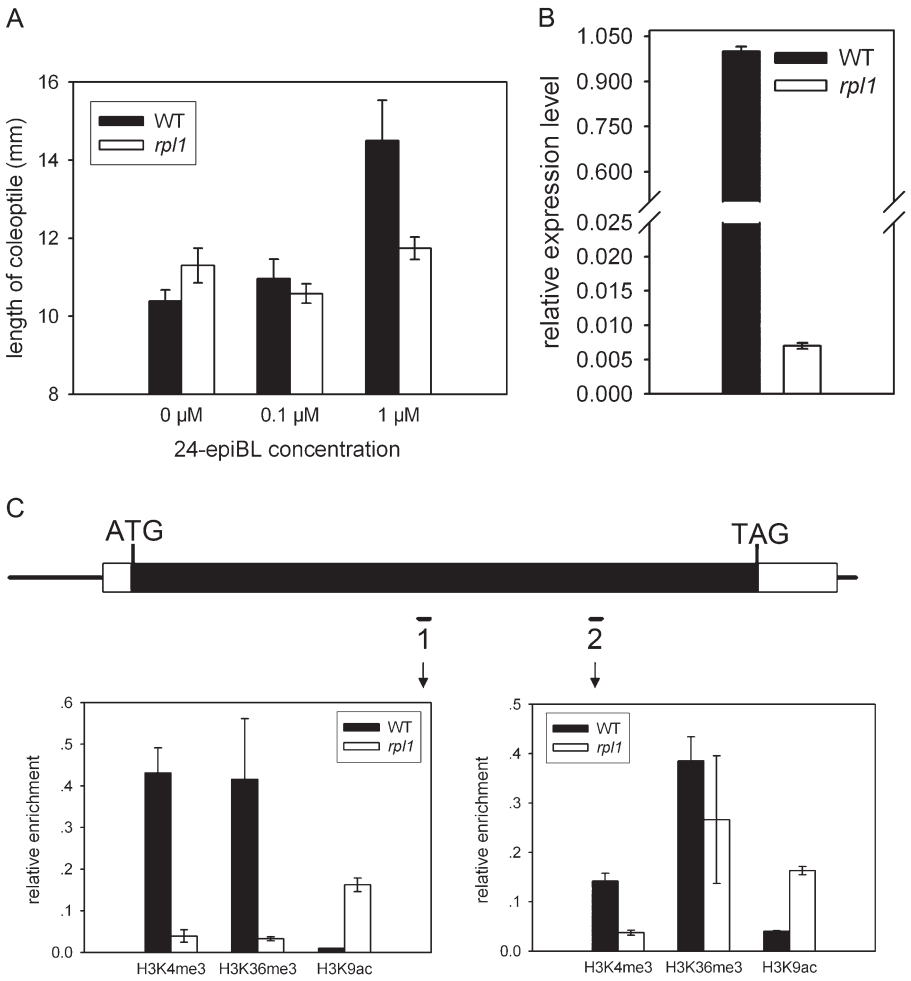

Figure 7. Response of *rpl1* Mutant to BR Treatment.

(A) Coleoptile length of seedlings grown in series concentration of 24-epiBL. Error bars, s.e.m., calculated from at least 28 seedlings.
(B) Quantitative RT–PCR analysis of *OsBRI1* in wild-type and *rpl1* seedlings. Error bars, s.e.m., based on three technical repeats.
(C) ChIP analysis of enrichment of histone marks at *OsBRI1*. Quantitative PCR analysis of relative enrichment of H3K4me3, H3K36me3, and H3K9ac in wild-type and *rpl1* seedlings. ChIP results were normalized to actin and then to the value of input DNA. Top panel, gene structure of *OsBRI1*, black box indicates exon, and white boxes indicate untranslated regions; black bars below indicate DNA fragments amplified. Bottom panel, results for fragment 1 and 2. Error bars, s.e.m., based on three technical repeats.

Plastic increases or decreases in stem elongation rate in plants could be triggered by light quality and quantity cues as well as mechanical stimuli (Cipollini and Schultz, 1999). It is known that phytohormones such as BR, and GA are involved in light-signaling to regulate plant growth (Alabadí and Blázquez, 2009; Feng et al., 2008; Luo et al., 2010; Sun et al., 2010). Our data on the *rpl1* mutant responses to BR GA, and CK and the greatly altered expression levels of the genes involved in the signaling of these hormones suggest that *RPL1* function in stability/plasticity control may involve hormone signaling. Moreover, the striking difference in height of mutant plants grown in Wuhan in summer, compared to in Lingshui in winter, and, in particular, the highly significant location-by-genotype interaction suggest that light quality, quantity, day length and/or temperature, singly or in combination, may all have contributed to phenotypic variations.

RPL1 Gene Is Involved in Epigenetic Processes in Regulating Phenotypic Plasticity

RPL1 was found to be localized in the nucleus. Areas of intense DAPI represented condensed, heterochromatic DNA (Brown et al., 1997). The GFP fluorescence from the GFP–RPL1 fusion protein showed a certain degree of overlapping with the DAPI-stained regions (Figure 3C), suggesting that the RPL1 protein might be involved with heterochromatin. The data showing that the mutation increased DNA methylation and altered histone modifications are in favor of the hypothesis that *RPL1* may be involved in epigenomic regulation of gene expression controlling plant growth.

The increase in DNA methylation in the mutant suggested that the RPL1 protein may have a function to repress DNA methylation. DNA methylation homeostasis appears to be important to plant height. The *Arabidopsis ddm1* mutant

showing decreased DNA methylation displays a reduced plant height after repeated self-pollination (Saze and Kakutani, 2007). The mutation of *Arabidopsis* ROS1 that functions as DNA glycosylase/lyase activity involved in DNA demethylation produces reduced plant height after selfing for four generations (Gong et al., 2002). In addition, knockdown or knockout of other chromatin modification or remodeling genes also affects plant height. Down-regulation of rice histone deacetylase genes *HDA710* and *HDA704* led to reduced plant height (Hu et al., 2009). RNAi lines of *Arabidopsis* chromatin-remodeling protein11 (*CHR11*), which constitutively lacked sporophytic *CHR11* activity, showed reduced plant height (Huanca-Mamani et al., 2005).

It has been shown that epigenetic processes contributed to environmentally induced phenotypic plasticity (Angers et al., 2010; Nicotra et al., 2010). Plant height was a key functional trait for research on plasticity and its underlying mechanisms (Nicotra et al., 2010). Environmental cues-induced alterations in stem growth can be mediated by plant hormones such as auxins, gibberellin, and ethylene (Cipollini and Schultz, 1999). In this study, we showed that *RPL1* may affect responses of the plant to gibberellin, brassinosteroid, and cytokinin signals by altering the epigenomic status of key hormone signaling genes such as *OsBRI1*. Thus, *RPL1* may regulate phenotypic plasticity through changing epigenomic status of components of phytohormone signaling.

RPL1 for Phenotypic Plasticity Is Important for Rice Evolution

Naturalists and geneticists have debated on the mechanism about the inheritance of acquired characters for decades. In 1942, Waddington coined 'canalization', which aided to understand it (Waddington, 1942). Canalization ensured the production of the normal and meant the resistance of developing organisms to change when perturbed genetically or environmentally (Pigliucci, 2002). Up to 2007, the HSP90 was the only described molecule with a canalization function (Salathia and Queitsch, 2007). Similarly to HSP90, whose mutation caused variable morphological phenotypes, the extent of plasticity increased when *RPL1* was disrupted. It indicated that *RPL1* limited phenotypic plasticity and acted as a factor for stable morphology resistant to environmental perturbation in rice, thus functioned as a capacitor other than the HSP90-buffering system.

The HSP90 family is highly conserved and organisms in all kingdoms of life except archaea have one or more genes encoding HSP90 (Taipale et al., 2010). However, the situation of RPL1 is very different. We searched all sequenced organisms with deduced peptide of RPL1 and found homologs only in plants (Query coverage $>$ 50%, E-value $<$ 1e-04). In plant species, we detected 14 predicted peptides or proteins in *Arabidopsis thaliana*, *Brachypodium distachyon*, *Glycine max*, *Medicago truncatula*, *Oryza sativa*, *Populus trichocarpa*, *Sorghum bicolor*, *Vitis vinifera*, or *Zea mays* showing a certain degree of homology to the *RPL1* deduced peptide (www.plantgdb.org/). Analysis of phylogenetic relationships showed that they had diverged into two clades (Supplemental Figure 3). All sequences from monocotyledon plants belonged to one clade and those from dicotyledon belonged to the other clade. The results suggested that RPL1 might be plant-specific, which regulates phenotypic variation only in monocot plants.

The origin and maintenance of phenotypic variation are a central theme in evolutionary biology, because adaptive phenotypic evolution depends on heritable variation in phenotypes (Sgro et al., 2010). The genetic and environmental effect on the amount and directions of genetic and phenotypic variation is of particular evolutionary importance because these constitute the materials to natural selection (Debat et al., 2009). Thus, reduced function of *RPL1* gene with increased phenotypic plasticity may potentially provide a larger range of phenotypes for natural and/or artificial selection, both in evolution and in plant breeding.

METHODS

Plant Materials and Growth Conditions

Wild-type, mutant, and transgenic plants were based on *Oryza sativa* ssp. *japonica* cv. Zhonghua11 background. All plants were planted under normal growth conditions in the experimental field of Huazhong Agriculture University at Wuhan or Lingshui, China.

Vector Constructions and Plant Transformation

5461 bp of genomic DNA fragment digested with *Sal*I and *Bam*HI from the BAC clone OSJNBa0073O11 containing intact *RPL1* gene coding sequence, 2161 bp upstream region of the initiation codon ATG, and 516-bp downstream region of the stop codon TAA were inserted into the binary vector pCAMBIA2301 for a complementation construct.

RPL1 cDNA fragments were amplified by PCR and directionally inserted into the transient expression vector pM999–ECFP or pM999–SUNLIGHTGFP. The constructs were transferred into protoplasts as described by Yoo et al. (2007) and observed using a confocal microscope. Transfected rice protoplasts expressing the RPL1–SUNLIGHTGFP fusion were stuck on glass slides and fixed in 2% paraformaldehyde in Phosphate Buffered Saline (PBS) then stained with DAPI, and the images were visualized using the confocal microscope.

BR, GA, and CK Treatments

For the treatment of BR, naked seeds were soaked in distilled water at 30°C for 2 d, and inoculated in ½ Murashige and Skoog-based media (0.15% phytagel) with Mock, 0.1 μM epiBL or 1 μM epiBL in constant darkness for 9 d. The length of coleoptiles of these seedlings was then measured.

To measure internode elongation in response to GA, seeds were sown in a pot of soil and grown to the three-leaf stage. The seedlings were used for hydroponic culture with

10^{-11}–10^{-4} M of GA_3 or without GA_3. After 4 weeks, total length of elongated internodes were measured.

To investigate the effect of exogenous cytokinin in crown root, 30 seeds for each genotype were sterilized and soaked in sterilized water at 30°C for 2 d. The seeds were placed on agar containing Mock, 5 or 15 μM kinetin, and incubated at 26°C under complete darkness. After 9 d of incubation, the number of crown roots was counted.

RNA Manipulation and qRT–PCR Analysis

Fresh plant tissues were harvested and immediately ground to fine powder in liquid nitrogen. For analyzing the expression pattern of *RPL1*, all samples were prepared from wild-type plants at the stage immediately before heading (panicle was about 22 cm long and was about to grow out of the sheath). For *OsBRI1* detection, shoots were sampled when they reached 1–2 cm. Total cellular RNA was prepared using a RNA extraction kit (TRIzol reagent, Invitrogen).

For RT–PCR, RNA samples were treated with DNaseI (Invitrogen) at 25°C for 15 min. The first-strand cDNA was synthesized using M-MLV reverse transcriptase (Promega) in 20 μl of reaction mixture containing 5 μg total RNA, according to the manufacturer's instructions. qRT–PCRs were performed in triplicate on an Applied Biosystems 7500 Real-Time PCR System as described (Xue et al., 2008). Primers were designed by PRIMER EXPRESS 3.0 software (PE Applied Biosystems). Data analyses with the $2^{-\Delta\Delta C_T}$ method were performed as described (Livak and Schmittgen, 2001). Actin gene was used as the internal reference.

In Situ Hybridization

The hybridization and immunological detection were performed as described by Xue et al. (2008). The *RPL1* probe was amplified using the gene-specific primers situ-F and situ-R (Supplemental Table 2). The PCR fragments were inserted into the pGEM-T (Promega) and transcribed *in vitro* from either T7 or SP6 promoter for sense or antisense strand synthesis using the Digoxigenin RNA labeling kit (Roche).

Western Blot Analysis

For Western blot analysis, histone proteins were extracted from wild-type or mutant seedlings as described (Tariq et al., 2003) and Western blot was prepared following Huang et al. (2007). The primary antibodies were purchased from Abcam (UK) and the secondary antibody (goat-anti-rabbit IgG) was from Invitrogen (USA). The following primary antibodies were used: antibodies against histone H3 (H3, ab1791), histone H3-acetylated K9 + K14 + K18 + K23 + K27 (H3ac, ab47915), histone H3-acetylated K9 (H3K9ac, ab4441), histone H3-monomethylated K9 (H3K9me1, ab8896), histone H3-dimethylated K9 (H3K9me2, ab1220), histone H3-trimethylated K9 (H3K9me3, ab8898), histone H3-dimethylated K27 (H3K27me2, ab24684), histone H3-monomethylated K4 (H3K4me1, ab8895), histone H3-dimethylated K4 (H3K4me2, ab32356), histone H3-monomethylated K36 (H3K36me1, ab9048), histone H3-dimethylated K36 (H3K36me2, ab9049), histone H3-trimethylated K36 (H3K36me3, ab9050).

ChIP Assay

For the ChIP assay, 2 g of shoots were prepared from wild-type and *rpl1* plants when the shoots were 1–2 cm long, and the assay was performed following a published method (Gendrel et al., 2005). The antibodies used were purchased from Abcam (Catalog No. ab12209 for H3K4me3, ab9050 for H3K36me3, and ab4441 for H3K9ac). Immunoprecipitated and input DNA was both analyzed by qRT–PCR as described above, and primers were designed by referencing the histone modification maps by He et al. (2010). Actin gene was used to normalize the immunoprecipitant ratio.

Bisulfite Sequencing

The DNA for bisulfite sequencing was extracted from seedlings 4 d after germination. The bisulfite treatment was performed using the EpiTect Bisulfite Kit from QIAGEN (catalog no. 59104). DNA purified from the kit was used as a template to amplify target DNA fragments. The PCR products were ligated into the pGEM–T vector (Promega) and electroporated into *E. coli* DH10B competent cells with selection on ampicillin containing plates. More than 20 clones were picked and cultured to extract plasmids for sequencing using the T7 primer. All sequence data were analyzed on the website http://katahdin.mssm.edu/kismeth.

SUPPLEMENTARY DATA

Supplementary Data are available at *Molecular Plant Online.*

FUNDING

This work was supported by grants from the 863 Project (SS2012AA100103) and the National Natural Science Foundation of China (30921091).

ACKNOWLEDGMENTS

We thank Professor Dao-Xiu Zhou for reading many earlier versions of this manuscript and giving helpful comments. The confocal images acquired with the Zeiss LSM 510 Meta confocal microscope were done with assistance of Yao Xiao in Ligeng Ma's lab at the National Institute of Biological Sciences, Beijing. We acknowledge Professor Jian Xu for the pM999–ECFP and pM999–SUNLIGHTGFP vectors. No conflict of interest declared.

REFERENCES

Alabadí, D., and Blázquez, M. (2009). Molecular interactions between light and hormone signaling to control plant growth. Plant Mol. Biol. **69,** 409–417.

Angers, B., Castonguay, E., and Massicotte, R. (2010). Environmentally induced phenotypes and DNA methylation: how to deal with unpredictable conditions until the next generation and after. Mol. Ecol. **19,** 1283–1295.

Brown, K.E., Guest, S.S., Smale, S.T., Hahm, K., Merkenschlager, M., and Fisher, A.G. (1997). Association of transcriptionally silent genes with Ikaros complexes at centromeric heterochromatin. Cell. **91,** 845–854.

Callahan, H.S., Pigliucci, M., and Schlichting, C.D. (1997). Developmental phenotypic plasticity: where ecology and evolution meet molecular biology. Bioessays. **19,** 519–525.

Cipollini, D.F., and Schultz, J.C. (1999). Exploring cost constraints on stem elongation in plants using phenotypic manipulation. Am. Nat. **153,** 236–242.

Debat, V., Debelle, A., and Dworkin, I. (2009). Plasticity, canalization, and developmental stability of the *Drosophila* wing: joint effects of mutations and developmental temperature. Evolution. **63,** 2864–2876.

Feng, S., et al. (2008). Coordinated regulation of *Arabidopsis thaliana* development by light and gibberellins. Nature. **451,** 475–479.

Gendrel, A.V., Lippman, Z., Martienssen, R., and Colot, V. (2005). Profiling histone modification patterns in plants using genomic tiling microarrays. Nat. Methods. **2,** 213–218.

Gong, Z., Morales-Ruiz, T., Ariza, R.R., Roldan-Arjona, T., David, L., and Zhu, J.K. (2002). *ROS1*, a repressor of transcriptional gene silencing in *Arabidopsis*, encodes a DNA glycosylase/lyase. Cell. **111,** 803–814.

Gutteling, E.W. (2004). Sense and Sensitivity: A Quantitative Genetic Analysis of Gene–Environment Interactions in Life History Traits in the Nematode. *Caenorhabditis elegans* (Wageningen: Print Partners Ipskamp).

He, G., et al. (2010). Global epigenetic and transcriptional trends among two rice subspecies and their reciprocal hybrids. Plant Cell. **22,** 17–33.

Hedden, P., and Phillips, A.L. (2000). Gibberellin metabolism: new insights revealed by the genes. Trends Plant Sci. **5,** 523–530.

Hirochika, H., Sugimoto, K., Otsuki, Y., Tsugawa, H., and Kanda, M. (1996). Retrotransposons of rice involved in mutations induced by tissue culture. Proc. Natl Acad. Sci. U S A. **93,** 7783–7788.

Hu, Y., et al. (2009). Rice histone deacetylase genes display specific expression patterns and developmental functions. Biochem. Biophys. Res. Commun. **388,** 266–271.

Huanca-Mamani, W., Garcia-Aguilar, M., Leon-Martinez, G., Grossniklaus, U., and Vielle-Calzada, J.P. (2005). CHR11, a chromatin-remodeling factor essential for nuclear proliferation during female gametogenesis in *Arabidopsis thaliana*. Proc. Natl Acad. Sci. U S A. **102,** 17231–17236.

Huang, L., Sun, Q., Qin, F., Li, C., Zhao, Y., and Zhou, D.X. (2007). Down-regulation of a *SILENT INFORMATION REGULATOR2*-related histone deacetylase gene, *OsSRT1*, induces DNA fragmentation and cell death in rice. Plant Physiol. **144,** 1508–1519.

Ikeda, A., et al. (2001). Slender rice, a constitutive gibberellin response mutant, is caused by a null mutation of the *SLR1* gene, an ortholog of the height-regulating gene *GAI/RGA/RHT/D8*. Plant Cell. **13,** 999–1010.

Jain, M., Tyagi, A.K., and Khurana, J.P. (2006). Molecular characterization and differential expression of cytokinin-responsive type-A response regulators in rice (*Oryza sativa*). BMC Plant Biol. **6,** 1.

Kakimoto, T. (2003). Perception and signal transduction of cytokinins. Annu. Rev. Plant Biol. **54,** 605–627.

Lehner, B., Crombie, C., Tischler, J., Fortunato, A., and Fraser, A.G. (2006). Systematic mapping of genetic interactions in *Caenorhabditis elegans* identifies common modifiers of diverse signaling pathways. Nat. Genet. **38,** 896–903.

Levy, S.F., and Siegal, M.L. (2008). Network hubs buffer environmental variation in *Saccharomyces cerevisiae*. PLoS Biol. **6** e264.

Liu, Z.L., et al. (2004). Activation of a rice endogenous retrotransposon *Tos17* in tissue culture is accompanied by cytosine demethylation and causes heritable alteration in methylation pattern of flanking genomic regions. Theor. Appl. Genet. **109,** 200–209.

Livak, K.J., and Schmittgen, T.D. (2001). Analysis of relative gene expression data using real-time quantitative PCR and the $2^{-\Delta\Delta CT}$ method. Methods. **25,** 402–408.

Luo, X.M., et al. (2010). Integration of light- and brassinosteroid-signaling pathways by a GATA transcription factor in *Arabidopsis*. Dev. Cell. **19,** 872–883.

Nicotra, A.B., et al. (2010). Plant phenotypic plasticity in a changing climate. Trends Plant Sci. **15,** 684–692.

Pigliucci, M. (2002). Developmental genetics: buffer zone. Nature. **417,** 598–599.

Pigliucci, M. (2003). Epigenetics is back! Hsp90 and phenotypic variation. Cell Cycle. **2,** 34–35.

Price, T.D., Qvarnstrom, A., and Irwin, D.E. (2003). The role of phenotypic plasticity in driving genetic evolution. Proc. R. Soc. Lond. B. **270**, 1433–1440.

Queitsch, C., Sangster, T.A., and Lindquist, S. (2002). Hsp90 as a capacitor of phenotypic variation. Nature. **417,** 618–624.

Rutherford, S.L., and Lindquist, S. (1998). Hsp90 as a capacitor for morphological evolution. Nature. **396,** 336–342.

Salathia, N., and Queitsch, C. (2007). Molecular mechanisms of canalization: Hsp90 and beyond. J. Biosci. **32,** 457–463.

Sangster, T.A., Queitsch, C., and Lindquist, S. (2003). Hsp90 and chromatin: where is the link? Cell Cycle. **2,** 166–168.

Saze, H., and Kakutani, T. (2007). Heritable epigenetic mutation of a transposon-flanked *Arabidopsis* gene due to lack of the chromatin-remodeling factor DDM1. EMBO J. **26,** 3641–3652.

Schlichting, C.D., and Smith, H. (2002). Phenotypic plasticity: linking molecular mechanisms with evolutionary outcomes. Evol. Ecol. **16,** 189–211.

Sgro, C.M., Wegener, B., and Hoffmann, A.A. (2010). A naturally occurring variant of *Hsp90* that is associated with decanalization. Proc. R. Soc. Lond. B. **277**, 2049–2057.

Sollars, V., Lu, X., Xiao, L., Wang, X., Garfinkel, M.D., and Ruden, D.M. (2003). Evidence for an epigenetic mechanism by which Hsp90 acts as a capacitor for morphological evolution. Nat. Genet. **33,** 70–74.

Sun, Y., et al. (2010). Integration of brassinosteroid signal transduction with the transcription network for plant growth regulation in *Arabidopsis*. Dev. Cell. **19,** 765–777.

Taipale, M., Jarosz, D.F., and Lindquist, S. (2010). HSP90 at the hub of protein homeostasis: emerging mechanistic insights. Nat. Rev. Mol. Cell Bio. **11,** 515–528.

Takano, M., Kanegae, H., Shinomura, T., Miyao, A., Hirochika, H., and Furuya, M. (2001). Isolation and characterization of rice phytochrome A mutants. Plant Cell. **13,** 521–534.

Takeda, K. (1977). Internode elongation and dwarfism in some gramineous plants. Gamma Field Sym. 1–18.

Tariq, M., Saze, H., Probst, A.V., Lichota, J., Habu, Y., and Paszkowski, J. (2003). Erasure of CpG methylation in *Arabidopsis* alters patterns of histone H3 methylation in heterochromatin. Proc. Natl Acad. Sci. U S A. **100,** 8823–8827.

Tirosh, I., Reikhav, S., Sigal, N., Assia, Y., and Barkai, N. (2010). Chromatin regulators as capacitors of interspecies variations in gene expression. Mol. Syst. Biol. **6,** 435.

Ueguchi-Tanaka, M., et al. (2000). Rice dwarf mutant *d1*, which is defective in the alpha subunit of the heterotrimeric G protein, affects gibberellin signal transduction. Proc. Natl Acad. Sci. U S A. **97,** 11638–11643.

Ueguchi-Tanaka, M., et al. (2005). *GIBBERELLIN INSENSITIVE DWARF1* encodes a soluble receptor for gibberellin. Nature. **437,** 693–698.

Vercelli, D. (2004). Genetics, epigenetics, and the environment: switching, buffering, releasing. J. Allergy Clin. Immunol. **113,** 381–386; quiz 387.

Via, S., Gomulkiewicz, R., De Jong, G., Scheiner, S.M., Schlichting, C.D., and Van Tienderen, P.H. (1995). Adaptive phenotypic plasticity: consensus and controversy. Trends Ecol. Evol. **10,** 212–217.

Vongs, A., Kakutani, T., Martienssen, R.A., and Richards, E.J. (1993). *Arabidopsis thaliana* DNA methylation mutants. Science. **260,** 1926–1928.

Waddington, C.H. (1942). Canalization of development and the inheritance of acquired characters. Nature. **150,** 563–565.

West-Eberhard, M.J. (1989). Phenotypic plasticity and the origins of diversity. Annu. Rev. Ecol. Evol. S. **20,** 249–278.

Wu, C., et al. (2003). Development of enhancer trap lines for functional analysis of the rice genome. Plant J. **35,** 418–427.

Xue, W., et al. (2008). Natural variation in *Ghd7* is an important regulator of heading date and yield potential in rice. Nat. Genet. **40,** 761–767.

Yamaguchi, S. (2008). Gibberellin metabolism and its regulation. Annu. Rev. Plant Biol. **59,** 225–251.

Yamamuro, C., et al. (2000). Loss of function of a rice *brassinosteroid insensitive1* homolog prevents internode elongation and bending of the lamina joint. Plant Cell. **12,** 1591–1606.

Yan, H., et al. (2010). Genome-wide mapping of cytosine methylation revealed dynamic DNA methylation patterns associated with genes and centromeres in rice. Plant J. **63,** 353–365.

Yoo, S.D., Cho, Y.H., and Sheen, J. (2007). *Arabidopsis* mesophyll protoplasts: a versatile cell system for transient gene expression analysis. Nature Protoc. **2,** 1565–1572.

Zhao, Y., Hu, Y., Dai, M., Huang, L., and Zhou, D.X. (2009). The WUSCHEL-related homeobox gene *WOX11* is required to activate shoot-borne crown root development in rice. Plant Cell. **21,** 736–748.